GL03320 GEOPHYSICS, VOL. 41, NO. 6 (DECEMBER 1976), P. 1318–1336, 4 FIGS., 4 TABLES

A DUAL-WAVELENGTH THERMAL INFRARED SCANNER AS A POTENTIAL AIRBORNE GEOPHYSICAL EXPLORATION TOOL

LEONARD A. LESCHACK* AND NANCY KERR DEL GRANDE‡

We are investigating a new airborne method for measuring surface temperatures that may be useful for identifying thermal anomalies of geologic origin. From Planck's equation we derive the valuable approximation that, for small temperature variations, the radiant emittance is proportional to the emissivity times the absolute temperature to the power of (50/wavelength in μm). From this, expressions are obtained for the emitted infrared (*ir*) radiation measured simultaneously in the 5 and 10 μm bands. Ratios of these expressions are shown to have the following useful properties at 288 K: (a) they are insensitive to surface emissivity variations for vegetated terrain, (b) they vary nearly as the 5th power of the surface temperature, and (c) they distinguish emissivity-related from temperature-related effects. We have made preliminary tests of this methodology at a field site in Scipio Center, New York. We have characterized the observed surface temperature variations, the significant effects of soil moisture, and separated out the purely emissivity-related features of vegetated terrain. Cluster analysis served to divide the *ir* data into groups that behave similarly as a function of the measured soil moisture. Two such distinct terrain groups were identified at the field site. The *ir* data were corrected for: (a) natural surface emissivity variations, (b) the intervening atmospheric path, and (c) the reflected sky radiation. The corrected surface temperature data were compared with calculated values computed from a model that simulates the surface temperature, using meteorological, hydrological, topographical, and soil thermal input parameters. The simulated mean surface temperatures, 291.9 K (group 1) and 291.[illegible] K (group 2), differed only by, respectively, 0.0 K and 0.1 K from the measured mean surface temperatures. Our preliminary results suggest the potential for developing a new airborne geophysical method for isolating abnormal heat flows. Weak heat flows, about 10–20 times the terrestrial average, have the effect of raising the surface temperature about 0.1–0.2 K. These temperature anomalies would, with the methodology suggested, appear as a residual difference between the *measured* (corrected) surface temperature and the *simulated* surface temperature. Such surface temperature differences appear, from our research, to be measurable by airborne *ir* scanners when data over surface areas of 0.1 km² or larger are averaged. Accordingly, our research appears to support the conclusion that surface temperature enhancements of geophysical origin between 0.1 and 0.2 K can be identified using airborne infrared methods.

INTRODUCTION

It has long been recognized that the measurement of geophysical parameters of the earth by airborne means can provide rapid and relatively inexpensive preliminary surveys of geologic prospects. Aerial magnetic and scintillometer surveys are examples that come to mind most immediately. Although other airborne geophysical measurements have been made with greater or lesser success, the airborne measurement of surface temperature appears to be fraught with complicating factors. On the other hand, rapid wide area mapping of surface temperatures would be very useful. A number of geologic phenomena worthy of com-

Manuscript received by the Editor January 20, 1976; revised manuscript received May 5, 1976.
* Development and Resources Transportation Co., Silver Spring, Md. 20902.
‡ Lawrence Livermore Lab., Livermore, Calif. 94550.

...vestigation are associated with the gen- ...of anomalous heat; the oxidation of ore ...d increased heat flow owing to potential ...al resources are examples. Accordingly, ...seem desirable to increase our com- ...of airborne geophysical methods to in- ...airborne measurement of minute surface ...ature differences.

...ring the time-dependent *true* surface ...ture from an aircraft and extracting the ...us and comparatively very small steady- ...mperature component of geologic origin is ...ognized as a complicated task. On the ...nd, mapping surface temperatures by air- ...rvey methods is an established technique. ...ualitative airborne infrared (*ir*) measure- ...made over geothermal anomalies by other ...ers have lent credence to the possibility ...easuring small surface temperature differ- ...from the air for geophysical exploration ...ently become feasible. Using an *ir* scanner ...e in the 3–5 μm range, Dickinson (1973) ...d evidence of new geothermal areas in ...New Zealand and delineated the extent of ...hydrothermal activity. Measurements of 0.5 ...K above ambient (Dickinson, personal ...munication, 1974) made at depths of 15 cm in ...areas outlined by the *ir* imagery con- ...d Dickinson's interpretation. In general, sur- ...emperature elevations of 1–3 K at Taupo, ...Zealand and 1–2 K at Mt. Amiata, Italy ...ter et al, 1973), outlined heat flow regions ...conductive components as small as 24–45 ...and convective components ranging to ...00 HFU. It is uncertain as to what percent- ...each component the scanners recorded dur- ...erflights. However, it is obvious from their ...that few or none of the temperature anoma- ...corded in the imagery were due solely to the ...of conductive heat flows, but rather to the ...ined effects of convective and conductive ...flows. The work of these researchers encour- ...us to investigate further the potential of air- ...e *ir* scanners as a geophysical tool and to ...particular emphasis on the possibility of ...ng quantitative measurements.

...r quantitative measurements, however, the ...tely sensed radiation must be corrected for ...effects of surface emissivity, meteorology, to- ...aphy, and surface material differences (Del ...nde, 1975) including thermal inertia and al- ...(Pohn et al, 1974), and particularly those ...to soil moisture (LeSchack et al, 1975) prior to obtaining any quantitative temperature measurement that could be useful for geophysical exploration. This paper discusses the theory of our approach to making quantitative temperature measurements and analyzes preliminary field data that support this theory. We found a number of references concerning the details of aerial infrared surveys of great value to our studies and they are included as general references.

DISCUSSION OF THEORY OF AIRBORNE TEMPERATURE MEASUREMENTS

As in the case of other geophysical exploration techniques, such as gravity or magnetic surveys, thermal surveys require the detection and isolation of a geologically induced field component that is only a small percentage of the overall field measured. For example, the cumulative extraneous effects that can mask temperature anomalies are often an order of magnitude greater than the sought-for anomalous component. Just as altitude, latitude, Bouger, and terrain corrections must be made to gravity data, and diurnal and normal corrections need to be applied to magnetic data, large corrections are necessary before useful interpretations can be made from airborne surface temperature data. There are three basic steps in isolating anomalous temperatures of geologic origin: (a) Measure the true surface temperatures over the survey area at a given time, (b) calculate the normal surface temperatures that would be anticipated for the same location and time, and (c) subtract the simulated temperature field from the measured temperature field to obtain a residual or anomaly field.

Measuring the true temperature

The first step in measuring the true temperature over a given geographical area is to record the radiant temperature over this area using a quantitative airborne infrared line scanner capable of sensing emitted energy at two wavelengths, at least. After the data have been recorded, we must then correct the calibrated radiant temperature data for: (a) variations in natural surface emissivity, (b) absorption and reemission in the atmospheric column between the surface and the scanner, and (c) reflected sky radiation due to the nonblackness of the terrain.

Estimating emissivity from ir *signal ratios*

It was recently shown (Del Grande, 1975) that the earth's surface radiates signals which for small temperature changes vary as the temperature T to the power $C_2/\lambda T_0$, where λ is the wavelength of the radiation, in *μm*, T_0 is the surface temperature in degrees Kelvin, and C_2 is a constant. At temperatures near 288 K, the spectral radiant emittance is proportional to the surface emissivity ϵ_λ times $T^{50/\lambda}$. This power law thermal model provides the physical rationale for ratioing narrow *ir* bands to produce signal ratios that are insensitive to the natural surface emissivity and have enhanced thermal responsivity. These signal ratios are used to obtain precise temperature measurements that are more easily identified with their geophysical origin. The derivation of this model, which is given in the Appendix, will be summarized below.

Planck's equation gives the hemispherical, spectral radiant emittance W_λ, measured in units of $(W \cdot m^{-2}/\mu m)$:

$$W_\lambda = \epsilon_\lambda C_1 \lambda^{-5} [(\exp C_2/\lambda T) - 1]^{-1}, \qquad (1)$$

where

W_λ = radiant emittance per unit wavelength at wavelength λ,
ϵ_λ = surface emissivity at wavelength λ,
C_1 = a constant, $3.7414 \times 10^8\ (W/m^2) \cdot \mu m^4$,
C_2 = a constant, $1.4388 \times 10^4 \mu m(K)$,
λ = wavelength in μm, and
T = surface temperature in K.

It is shown in the Appendix that (1) may be approximated as follows:

$$W_\lambda(T) = C_\lambda(T_0)(T)^{C_2/\lambda T_0} \propto \epsilon_\lambda T^{C_2/\lambda T_0}, \qquad (2)$$

with $C_2 = 14388\ \mu m \cdot K$ and a nominal value of $T_0 = 288$ K, $C_2/T_0 = 49.96$, equation (2) can be closely approximated by:

$$W_\lambda = C_\lambda(T_0)\, T^{50/\lambda} \propto \epsilon_\lambda T^{50/\lambda}. \qquad (3)$$

Accordingly, we have derived a convenient expression for calculating the temperature sensitivity of aerial infrared scanning systems. At a typical predawn temperature of 288 K, we see from equations (1) and (3) that the detectable radiation emitted over the wavelength band and centered at λ is proportional to $\epsilon_\lambda T^{50/\lambda}$.[1] Filters are used to define narrow bands. A few bands avoid both atmospheric absorption regions and wavelengths associated with anion groups in common minerals where the terrain behaves as a spectral source. These bands are centered at 2.2, 3.5, 3.9, 4.8, and 13.2 μm. At these wavelengths, the signal responses vary, respectively, approximately as the 23rd, 14th, 13th, 10th, and 4th power of the absolute temperature.

The earth's emissivity is highly variable from one location to the next. However, the ratio of signals at two or more wavelengths can be used to obtain accurate surface-temperature measurements that depend very little upon emissivity variations. For two bands at wavelengths λ_1 and λ_2, the temperature response of the signal ratio is:

$$\frac{W_{\lambda_1}}{W_{\lambda_2}} = \frac{\epsilon_{\lambda_1}}{\epsilon_{\lambda_2}} \frac{T^{C_2/\lambda_1 T_0}}{T^{C_2/\lambda_2 T_0}}. \qquad (4)$$

Variations in the emissivity ratio are smaller by a factor of ten or more than variations in the absolute emissivity for different natural terrains. At wavelengths where the radiation has the same spectral slope as a blackbody source, the emissivity ratio variations are very small. Thus, quantitative temperature measurements can be made, using signal ratios that are calibrated against a standard blackbody source.

Where the surveyed terrain behaves in true graybody fashion, i.e., no matter what material is scanned in the survey, the ratio of $\epsilon_{\lambda_1}/\epsilon_{\lambda_2}$ is constant, then the ratio of two signals of differing wavelengths can be calibrated and the blackbody temperature obtained. In this work we let $\lambda = 5$ μm and 10 μm, respectively, because these are the common wavelengths that are recorded by present-day scanners and, as such, are the wavelengths in which our field data were obtained. However, energy radiated in the 10 μm band does not generally exhibit graybody behavior (Del Grande, 1975) so that for future surveys another wavelength, e.g., 13.2 μm, would be more appropriate. On the other hand, as discussed below, where the terrain surface is covered by vegetation, radiation in the 10 μm band does appear to behave in a graybody fashion. This permits us to develop the following relationships which apply at about 288 K, a nominal field value for the surface blackbody temperature T_b from equation (4):

$$\frac{W_5}{W_{10}} = \frac{\epsilon_5 T_b^{10}}{\epsilon_{10} T_b^{5}}, \qquad (5)$$

and

$$\left(\frac{W_5}{W_{10}}\right)^{1/5} = \left(\frac{\epsilon_5}{\epsilon_{10}}\right)^{1/5} T_b. \qquad (6)$$

[1] We note that the commonly used temperature power law is T^4 (resulting from Stefan-Boltzmann's equation). This describes the temperature response of the *total* radiant emittance [i.e., the integral of equation (1) over all wavelengths] as well as for a band centered near 12.5 μm.

...plies that by ratioing the 5 and 10 μm ...d calibrating the resulting signal, a di- ...surement of T_b, the blackbody temper- ...n be obtained. For the specific problem ...ating the emissivity necessary to correct ... which was calibrated assuming a black- ...rce, the following relationships are ob- ...om equation (3):

$$T_{10} \propto W_{10}^{\lambda/50} \propto \epsilon_{10}^{1/5} T_b, \tag{7}$$

$$T_5 \propto W_5^{\lambda/50} \propto \epsilon_5^{1/10} T_b. \tag{8}$$

...ng equations (7) and (8) to the 10th power ...oing them, we derive the following ex- ...n for the surface emissivity ϵ_{10}:

$$\left(\frac{T_{10}}{T_5}\right)^{10} \propto \frac{\epsilon_{10}^{2}}{\epsilon_5} \propto \epsilon_{10}. \tag{9}$$

...n (9) holds for vegetated surfaces which ... graybody behavior at 5 and 10 μm, i.e., the ... ϵ_λ for these surfaces is constant. We have ...ed that graybody behavior does pertain to ...faces that we have measured since they ...egetation covered, and from the data of ...nd Tantraporn (1952) it can be shown that ... ϵ_{10}/ϵ_5 for 40 different vegetation samples ...nt to better than one percent. This implies ...hough ϵ_{10}/ϵ_5 is not necessarily unity, it ...nstant for a variety of different vegetation ...nd, thus, can be determined by calibration ...ces.

...lytical and physical basis for atmospheric ...ons

...spheric corrections for radiant temper- ...easurements must be made both for the ...ion and emission in the intervening air ...etween the surface and the scanner) and ...e reflected sky radiation due to the non- ...ss of the terrain.

... (1974) has established the physical and ...al basis for these corrections. Near the ...the radiant emittance W_g is the sum of the ...d surface radiation and the reflected sky ...on:

$$W_g = \epsilon_\lambda W_b + (1 - \epsilon_\lambda) W_s. \tag{10}$$

...bscripts g, λ, b, and s refer, respectively, to ...diated (graybody) temperature at the sur- ...he wavelength band, the directly measur- ...lackbody) surface temperature, and the temperature associated with the sky and cloud cover. The emissivity is given by ϵ_λ and the reflectance coefficient by $1 - \epsilon_\lambda$.

At some distance h, above the terrain, the measured radiant emittance W_h consists of the transmitted surface radiance and the emitted radiance of the intervening column of air. Thus,

$$W_h = W_g (1 - A) + W_a A. \tag{11}$$

The subscript a refers to the temperature of the air column. Most previous studies approximate the temperature of the air column as the value measured for the air temperature outside the aircraft at the altitude of the scanner. These studies will be used to estimate a value for A, the absorption or emission of the air column appropriate for the conditions of our experiment to be discussed below.

Tien (1974) shows that by eliminating W_g, together with appropriate algebraic manipulations, equations (10) and (11) can be combined as follows:

$$W_b - W_h = \frac{1}{\epsilon_\lambda}\left(\frac{A}{1 - A_\lambda}\right)(W_h - W_a) + \left(\frac{1 - \epsilon_\lambda}{\epsilon_\lambda}\right)(W_h - W_s). \tag{12}$$

He further applies a two-term truncated Taylor series expansion of the $W(T)$ around $W_h\,(T_h)$ on both sides of equation (12):

$$W(T_h + \Delta T) \simeq W_h(T) + \Delta T W'_h(T_h). \tag{13}$$

By canceling out terms of the form $W_h\,(T_h)$, and dividing both sides of the subsequent equation by $W_h\,(T_h)$, he obtains:

$$T_b - T_h \approx \frac{1}{\epsilon_\lambda}\left(\frac{A}{1 - A_\lambda}\right)(T_h - T_a) + \left(\frac{1 - \epsilon_\lambda}{\epsilon_\lambda}\right)(T_h - T_s). \tag{14}$$

This approximation is valid when the temperature correction is small compared to the absolute surface temperature, as is typically the case. Equation (14) is in agreement with the experimental observations reported previously by Weiss (1971), Saunders (1970), and Shaw and Irbe (1972). Most of these measurements were made over ocean surfaces which had an emissivity of 0.986 near 10 μm. Equation (14) permits us, therefore, to correct directly for the blackbody temperatures at the earth's surface.

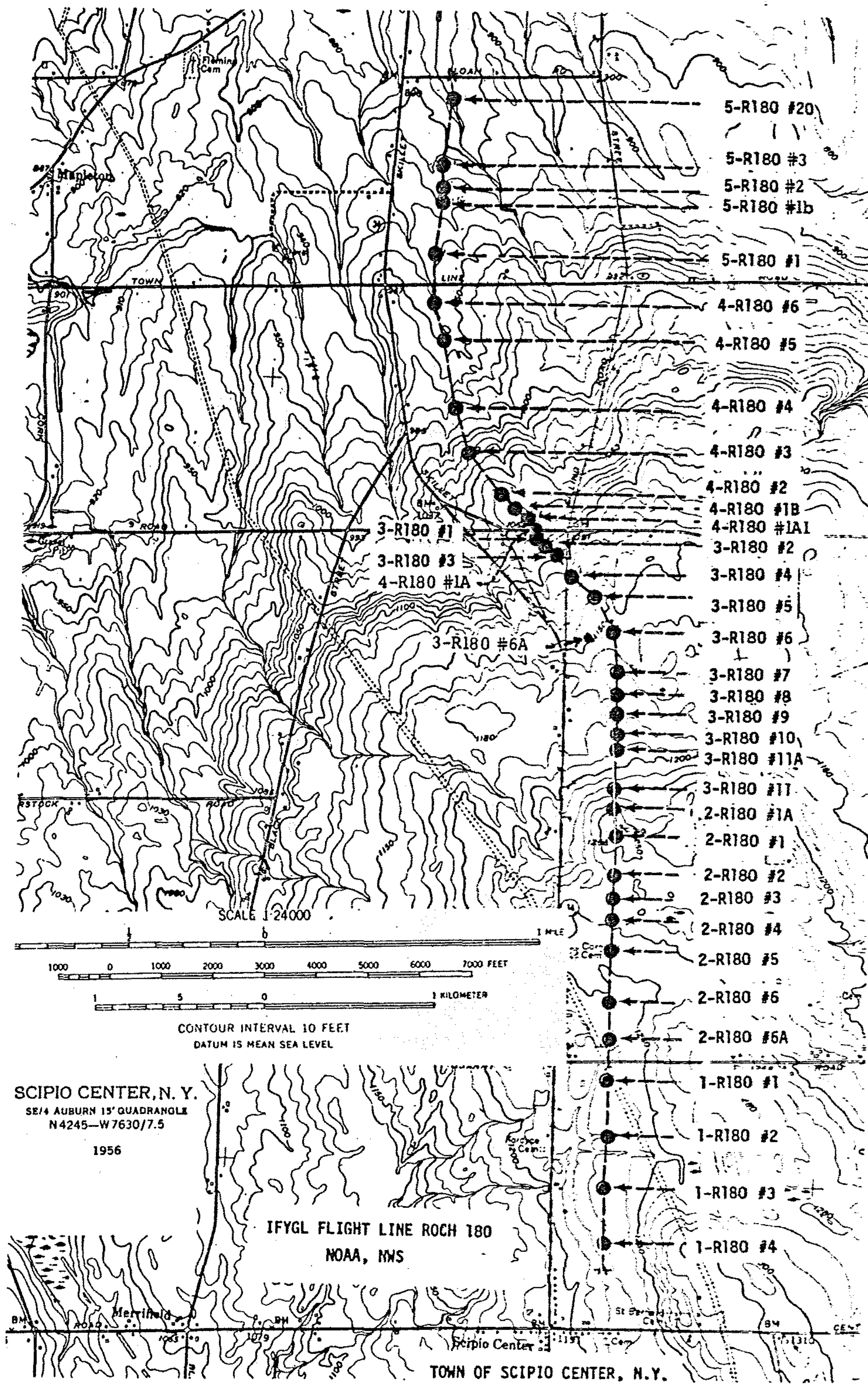

FIG. 1. Locations of soil sample sites (after Peck et al, 1972).

2. Digicolor images of Scipio Center, N.Y. site (see Figure 1). 10 μm image on left, 5 μm image on ... The radiant temperatures range as follows: white = all above 59°F; red = 58°–59°F; yellow = ...–58°F; green = 56°–57°F; cyan = 55°–56°F; blue = 54°–55°F; magenta = 53°–54°F; black = all ...ow 53°F.

1324
blank

-ory, the above steps take the raw but ...ed radiant temperature data obtained as ...from the scanner, make approximate cor-...to them for variations in surface emissiv-... finally, enable corrections for the atmo-...olumn to be made. A map of such surface ...tures, although perhaps accurate for the ...of time during which the data were re-... is, however, transitory. Our next step, ...re, is to calculate, on a point-by-point basis ...same survey area, the "normal" surface ...atures (i.e., the temperatures that would be ...ed under equilibrium conditions due to all ...mental causes other than abnormal heat ... We accomplish this with a digital equilib-...urface temperature simulator model.

...ting the "normal" surface temperature

...calt (1972a, b, c, d) has demonstrated the ...ation of an equilibrium surface temperature ...tor to predict, with reasonable accuracy, ...oretical surface temperature for any given ...on the terrain. The precision of the model is ...ntly adjusted to a threshold of 1 mly · min^{-1} ... to 17 HFU)[2] and this threshold could be ...er reduced. Outcalt (1972b) has shown that ...model is sufficiently accurate to replicate sur-...temperature differences on the order of ±0.2 ...sociated with different types of terrain as ...ured by airborne *ir* surveys.

...calt (1972b) describes the model as follows:[3]

> In brief, the operation of the general sim-...ator is based upon the energy con-...rvation equation which states that the ...ur components of the energy budget (net ...diation R, soil heat flux S, sensible heat ...x H, and latent heat flux L) must have a ...ero sum across a surface:
>
> $$R + S + H + L = 0 \qquad (1)$$
>
> In turn each of these terms is a complex ...nction of the environmental variables which specify the radiation and thermal ...roperties of the atmosphere and substrate ...edia. At any instant in time these com-...ponents may be represented as functions of ...a limited set of environmental variables and physical constants. These controlling varia-...bles are listed with their notation in Table 1.
>
> The components of the energy budget equations can then be written in terms of these variables and the surface temperature (T) as
>
> $$R = f(LAT,\ DEC,\ D,\ R,\ ALBEDO,\ W,\ P,\ TSKY,\ T) \qquad (2)$$
>
> If the assumption is made that the soil temperature at the diurnal damping depth is approximately equal to the mean air temperature, then
>
> $$S = f(GEC,\ GD,\ TA,\ T) \qquad (3)$$
>
> The turbulent transfer terms which are corrected for stability using the Richardson number may be expressed as
>
> $$H = f(U,\ ZO,\ P,\ TA,\ T), \qquad (4)$$
>
> $$L = f(U,\ ZO,\ P,\ RH,\ SRH,\ TA,\ T) \qquad (5)$$

Table 1. Environmental input variables

Station pressure (P)	Mean air Temperature (TA)
Latitude (LAT)	Mean Air Relative humidity (RH)
Solar declination (DEC)	Mean wind speed (U)
Dust particles cm^{-3} (D)	Soil thermal diffusivity (GD)
Orbital radius vector (R)	Soil volume Heat capacity (GC)
Surface Albedo (ALBEDO)	Surface roughness length (ZO)
Precipitable water (W)	Soil surface wetness (SRH)
Sky radiant temperature ($TSKY$)	

> Note that in all of the above equations after specification of the input variables the surface temperature is the only unknown. The soil temperature profile is allowed to evolve by calculating a finite-difference solution from the preceding step. After the new soil thermal profile is calculated, the soil heat flux [equation (3)] is actually calculated from the uppermost soil temperature level in place of TA.
>
> At each step through the diurnal cycle the solar radiation incident on a surface may be calculated for a clear day by means of a subroutine. Subroutines are also included to calculate specific humidity gradients, to fix the free air computation level, and to correct the thermal properties of the atmosphere for stability.
>
> It is apparent that if a sequence of guesses as to the value of the surface temperature are entered into the equation the correct guess would bring the energy budget equation [equation (1)] to zero; that correct guess would be termed the equilibrium surface temperature. The equilibrium surface temperature is that temperature guess which produces a suitably small residual in the energy budget equation (e.g., 1 mly min^{-1}). Then all the components of the energy transfer regime (R, S, H, L) and the soil temperature vector are equally good

[2] HFU = 1 μ cal·cm^{-2}·S^{-1} = 0.042 W·m^{-2}.

[3] Reprinted by permission of the American Meteorological Society.

guesses, and the next iteration begins with a forward solution of the finite-difference form of the soil thermal diffusion equation.

The output of this model is the absolute temperature as a function of solar time for each survey point. It can be seen that if the theoretical point-by-point temperatures as computed from the above model are subtracted appropriately from the temperature data array that would be generated from the procedures previously described, the residual should be the thermal anomaly field sought.

ANALYSIS OF PRELIMINARY FIELD DATA

On 11 October 1972, soil moisture data were collected along a 7 km line near Scipio Center, New York, while concurrent 4.5–5.5 μm airborne *ir* data were recorded at an altitude of 2000 m above mean sea level (Peck et al., 1972). These data, along with simultaneous multiband photographs, were gathered by the National Oceanic and Atmospheric Administration in conjunction with the International Field Year for the Great Lakes program. These data, recorded over an area presumed to have no abnormal heat flow, were used to make a preliminary test of our theoretical approach to airborne surface temperature measurements discussed above. Adequate information derived from these measurements, from local National Weather Service records, and from the literature permit obtaining the arguments outlined in Table 1 needed to evaluate the surface temperature simulator.

Data collection

A Daedalus Enterprises Dual Channel Scanner, model DS 1230, was used to gather simultaneously the 4.5–5.5 μm and 8–12 μm data.[4] The flight line (no. 1.1) was flown in a north-south direction over the study profile line. The profile line parallels Skillet Road and is offset 300 m ($\pm$25 m) to the east of it (Figure 1). The airborne data were gathered at an altitude of 1700 m above mean terrain on 11 October 1972 at 1527 hours local solar time [1519 hours local mean time (EST)].

The weather was sunny with high cirrus and scattered altocumulus clouds and 20-mile visibility. The ambient air temperature was 11°C at 1 m above the ground surface. The mean wind speed was 10 knots. Soil samples were taken from 10 cm beneath the surface by auger. The soil moisture percent by weight in each core sample was determined later. A general description of the vegetation was made at each soil sampling site. Specific soil data were not collected, but general descriptions can be obtained from Soil Conservation Service maps.

The *ir* data were recorded simultaneously in the 5 and 10 μm wavelengths on magnetic tape. Calibrated digitized images were then prepared.[5] The quantitative "Digicolor" format presents the radiant emittance data as six discrete levels, each level corresponding essentially to a 1°F (= 0.6°C) change of blackbody temperature from 53°F to 59°F (11.7°C-15.0°C). The calibration is established by two blackbody reference sources that are an integral part of the IR scanner used for this work. The blackbody reference sources are adusted so as to straddle the radiant temperature values observed in the given airborne mission. For the Scipio Center flight line, reference values of 10°C and 20°C were used. The blackbody reference sources are calibrated in the laboratory before each mission by scanning, in the 10 μm range, a water bath[6] 1 m from the scanner. The temperature of the water bath is varied from 5°C to 40°C in 2 degree steps. The radiant emittance data recorded by the scanner can, therefore, be divided into discrete levels corresponding to calibrated blackbody temperatures. This does not imply that these are the exact or directly measurable ground surface temperatures, but rather the radiant ground surface temperatures modified by (a) the surface emissivity, (b) the absorption and reemission of the intervening air column between the scanner and the ground, and (c) the sky radiation reflected from the ground. These effects must be corrected as discussed above.

Quantifying the calibrated Digicolor images

The calibrated radiant emittance data are presented as images on 70 mm color film (Figure 2). Each 1°F (0.6°C) level of radiant temperature from 53°F (11.7°C) to 59°F (15.0°C) is displayed in a different color. Everything lower than 53°F (11.7°C) is black and everything higher than 59°F (15.0°C) is white. The 70 mm Digicolor film strips for both the 5 μm and 10 μm wavelengths were optically enlarged to convenient dimensions and the soil profile line was overlain on the imagery. The radiant temperature values along the profile line were then recorded.

[4] Mean values, i.e., 5 μm and 10 μm will be used for simplicity in the discussion that follows.

[5] Digicolor Images by Daedalus Enterprises, Inc. presented on 70 mm color film.

[6] The water is presumed to have an emissivity ϵ of 1

...ble 1. Emissivity (ϵ) of common vegetation (after Wolfe, 1965)

	3–5 μm	8–13 μm
...ntain laurel	= 0.90	= 0.92
...ow leaf (dry, top)	0.94	0.96
... (dry, top)	0.90	0.90
... (dry, bottom)	0.86	0.94
...rmant maple leaf (dry,	0.87	0.92
...f winter color—oak		
...ry, top)	0.90	0.92
...iferous twigs (jack pine)	0.96	0.97
...eadow fescue (dry)	0.82	0.88
...orthern red oak	0.90	0.96
...North American jack pine	0.88	0.97
...Colorado spruce	0.87	0.94

...mination of Figure 1 shows that the data ... support our theory is taken over an area ... at 10 km². In a typical regional geophysical ... an area of this size would generally con... ...ly a few data points representing in... ...ons of the field around them. Since a cluster ...s technique divided our 38 data samples ...o natural terrain groups (group 1 having ...or dying vegetation, group 2 having live ...ation) (LeSchack et al, 1975), we elected to ...e mean values of temperature associated ...each group as an appropriate integrated ...e for comparison for a residual anomaly ... Accordingly, our tabulations of observed ...culated temperatures will be listed follow... ...s grouping.

Radiant temperature data corrections

Emissivity corrections can be directly estimated when the emissivity ratio (in this case ϵ_{10}/ϵ_5) is constant. From equation (9) we obtain the following:

$$\left(\frac{T_{10}}{T_5}\right)^{10} = k\epsilon_{10} \propto \epsilon_{10}, \qquad (15)$$

where k is a constant.

Then, using equation (15) we determine surface emissivity values at 18 locations in group 1 and 16 locations in group 2. The constant of proportionality k for these two groups was determined from published data. The mean value of ϵ_{10} for 11 vegetation types (Table 1) cited by Wolfe (1965) is equal to 0.935. We assumed ϵ_{10} for our data groups had the same mean value, and obtained the following equations from which the emissivity values were determined.

Group 1

$$\epsilon_{10} = .9593\left(\frac{T_{10}}{T_5}\right)^{10}. \qquad (16)$$

Group 2

$$\epsilon_{10} = .9582\left(\frac{T_{10}}{T_5}\right)^{10}. \qquad (17)$$

The emissivity values for each location along with

Table 2. Group 1—temperature data for dry vegetation-covered areas.

...ation	Soil moisture, percent	T_b K	T_c K	ϵ_{10}	$\left(\frac{.3228}{\epsilon_{10}}\right) \times (T_{10} - 277.0)$	$\left(\frac{1-\epsilon_{10}}{\epsilon_{10}}\right) \times (T_{10} - 260.7)$	T_5 K	T_{10} K
[illegible]	38.1	292.5	290.2	.939	3.5	1.7	287.9	287.3
[illegible]	36.6	292.7	293.0	.914	3.5	2.4	288.2	286.8
[illegible]	34.9	293.0	291.4	.907	3.5	2.7	288.4	286.8
[illegible]	32.6	292.5	293.1	.939	3.5	1.7	287.9	287.3
[illegible]	31.8	293.2	290.4	.934	3.7	1.9	288.4	287.6
[illegible]	31.8	292.5	289.8	.939	3.5	1.7	287.9	287.3
[illegible]	31.8	292.3	292.9	.924	3.4	2.1	287.9	286.8
[illegible]	31.7	293.0	291.2	.907	3.5	2.7	288.4	286.8
[illegible]	31.5	291.0	289.9	.939	3.2	1.6	286.8	286.2
[illegible]	28.8	292.5	290.0	.939	3.5	1.7	287.9	287.3
[illegible]	28.6	291.0	292.9	.939	3.2	1.6	286.8	286.2
[illegible]	28.5	291.5	293.5	.924	3.2	2.1	287.3	286.2
[illegible]	27.8	291.0	292.5	.939	3.2	1.6	286.8	286.2
[illegible]	25.4	291.0	289.9	.939	3.2	1.6	286.8	286.2
[illegible]	24.4	291.5	292.7	.924	3.2	2.1	287.3	286.2
[illegible]	23.6	291.8	293.5	.942	3.4	1.6	287.3	286.8
[illegible]	20.5	290.7	292.4	.997	3.3	0.1	286.2	287.3
[illegible]	16.4	290.2	294.3	.942	3.0	1.5	286.2	285.7
...n value	29.2	291.88	291.87	.935	3.4	1.8	287.47	286.72
...dard ...viation	5.5	.92	1.51	.019	0.2	0.6	0.71	0.53

Table 3. Group 2—temperature data for green vegetation-covered areas.

Location	Soil moisture, percent	T_b K	T_c K	ϵ_{10}	$\left(\frac{.3228}{\epsilon_{10}}\right) \times (T_{10} - 277.0)$	$\left(\frac{1-\epsilon_{10}}{\epsilon_{10}}\right) \times (T_{10} - 260.7)$	T_s K	T_{10} K
41a1	46.3	293.0	290.0	.913	3.5	2.5	288.4	287.0
1-1	43.6	291.8	289.3	.942	3.4	1.6	287.3	286.8
4-1a	38.0	292.5	291.4	.939	3.5	1.7	286.5	286.2
1-2	34.2	290.7	289.9	.948	3.1	1.4	286.5	286.2
2-6	34.1	290.7	292.6	.948	3.1	1.4	286.5	286.2
1-4	33.4	290.8	291.8	.922	3.0	2.1	286.8	285.7
3-1	32.8	291.6	293.4	.922	3.2	2.2	287.3	286.2
3-8	29.2	292.5	290.8	.939	3.5	1.7	287.9	287.3
4-1b	29.2	291.5	293.2	.912	3.2	2.4	287.3	285.9
3-11a	28.9	291.6	291.8	.922	3.2	2.2	287.3	286.2
3-7	28.0	292.5	293.3	.929	3.5	2.0	287.9	287.0
3-11	28.0	290.3	290.7	.948	3.0	1.4	286.2	285.9
3-10	27.5	292.5	292.9	.929	3.5	2.0	287.9	287.0
2-5	26.4	289.4	291.6	.967	2.9	0.8	286.2	285.7
2-1a	26.4	291.3	291.0	.932	3.2	1.9	287.0	286.2
2-3	20.9	290.7	292.0	.948	3.1	1.4	286.5	286.2
Mean value	31.7	291.46	291.61	.935	3.2	1.8	287.18	286.42
Standard deviation	6.4	0.99	1.27	.014	0.2	0.4	0.67	0.53

the soil moisture, the radiant temperatures, the blackbody temperatures and the calculated "normal" temperatures are listed in Table 2 (for the group 1 data) and Table 3 (for the group 2 data).

Whereas the published data for ϵ_{10} ranged from 0.88 to 0.97 and had a standard deviation of 0.028, our data ranged from 0.907 to 0.997 with a standard deviation of 0.019 (for group 1) and from 0.912 to 0.967 with a standard deviation of 0.014 (for group 2). The emissivities that we have derived based on (a) the calibrated radiant temperature values, (b) the power law thermal model, and (c) the assumption of a mean value for ϵ_{10} equal to 0.935, appear to be in agreement with measurements made by Hodder (personal communication, 1974). They have a slightly lower average emissivity than the value 0.963, calculated from the data taken by Gates and Tantraporn (1952). Without field measurements of the emissivities at specific locations, the possibility exists that the mean emissivity value at 10 μm may be as much as 3 percent higher.

Corrections for the atmospheric column, equation (14), embodies the analytical technique that we use to obtain the true surface temperature at each point. Rewriting this equation gives us the difference between the surface blackbody temperature T_b for the vegetated terrain and the measured radiant temperature T_h, given by the calibrated radiant temperature T_{10} in our experiment:

$$T_b - T_{10} \approx \frac{1}{\epsilon_{10}}\left(\frac{A_{10}}{1 - A_{10}}\right)(T_{10} - T_a) + \left(\frac{1 - \epsilon_{10}}{\epsilon_{10}}\right)(T_{10} - T_s). \quad (18$$

The first term on the right-hand side character izes the temperature correction for the intervenin atmospheric air path. According to the empirica results of Weiss (1971), the temperature decreas $(T_{10} - T_a)$ for an air column of 1700 m is 9.73°C Consequently we let T_a = 277.0 K which is 9.73°C lower than the mean value of T_{10} (for group 1) The absorption coefficient A_{10} was determined t be 0.244, based on the empirical results reporte by Saunders (1970) corrected to meet the condi tions of our experiment. The coefficient A_{10}, whic depends on atmospheric absorption and reemis sion, is a function of the water vapor mixing ratio which we took as 3.5 gm/kg for a relative humid ity of 48 percent. Given a 300 m path, Saunder (1970) computes the effective absorption A_{10} a 0.082 for this mixing ratio. We corrected (linearly for a path of 1700 m, and reduced the coefficien to compensate for our experimental filter, whic had a narrower detection band (about 8-12 μm compared to the 8-15 μm used by Saunders). Th latter effect reduces the value of A_{10} by a factor o about 1.9 or less, based on the results of studie made by Weiss (1971). We believe the value take for A_{10}, based on simplified assumptions for th longer column of air and for the different detec tion filter, could be as much as 20 percent highe than the value used in our calculations. Withou field measurements to verify this atmospheric pa

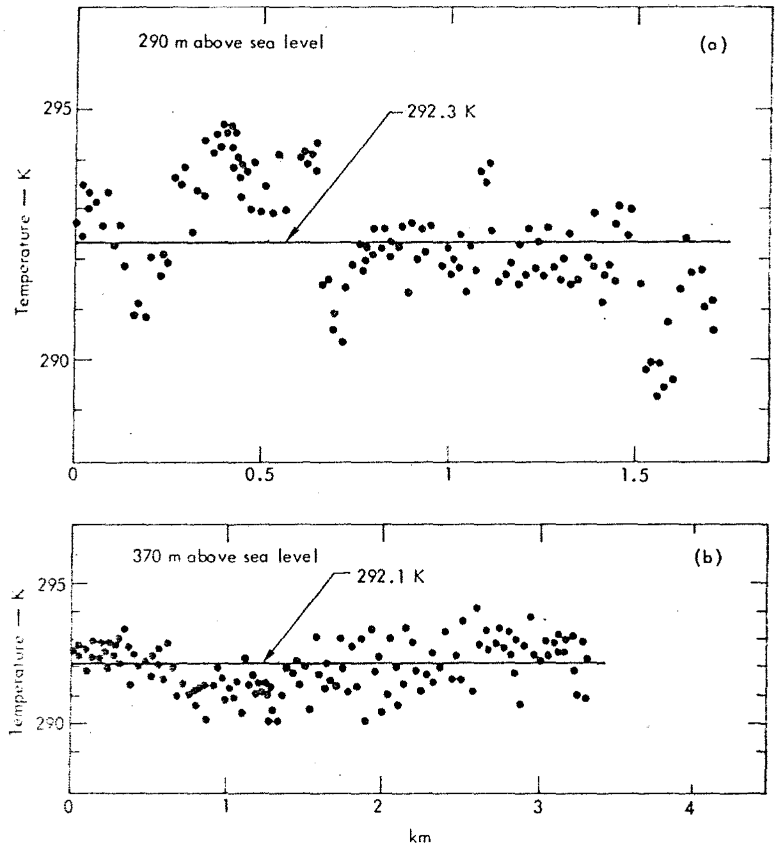

3. Corrected surface temperature measurements from ratios of dual-band infrared surveys at 5 and ... over vegetated terrain. The data for small areas of about 300 m² vary from the mean as much as 2 ... 1527 solar time. By smoothing the data, the average temperatures for large areas of 70,000 (curve ... and 160,000 (curve b) m² were found to differ by 0.2 ± 0.1 K. This difference mainly resulted from ... normal temperature drop with increasing altitude. Taken from Del Grande (1975).

...ever, we must include this possibility in our subsequent discussion of errors.

The second term on the right-hand side of equation (18) characterizes the temperature correction for the reflected sky radiation from a nonblack surface. The average sky temperature, contributing to this effect T_s, was taken at 260.7 K to represent the conditions during the survey.

...corrected surface temperature data

A summary of the data and temperature corrections is given in Tables 3 and 4. The location of the data positions, the percentage soil moisture, the corrected surface temperature, and the calculated surface temperature (discussed below) are given in the first four columns. Also included are the emissivity values ϵ_{10} calculated from equations (16) and (17) and the temperature corrections for the atmospheric path and the reflected sky radiation from equation (18). The uncorrected radiant temperatures at 5 μm and 10 μm are given for purposes of comparison. The mean value and standard deviation are calculated for each of these parameters.

We note surprisingly good agreement between the correct mean experimental surface temperature T_b and the calculated mean surface temperature T_c, based on our model that is discussed below. For group 1 (dry vegetation), the experimental value for the mean is 0.01 K higher than the calculated value; for group 2 (green vegetation), the experimental value is 0.15 K lower than the calculated value.

The standard deviations calculated from the data are for each measurement somewhat less than the corresponding standard deviations based on our model. There are two known effects which would contribute to this. First, the dispersion associated with partitioning the calibrated radiant temperature data into discrete temperatures, each separated by about 0.6 K, does not reflect the natural dispersion. Second, the surfaces with lower than average emissivities cool less efficiently since they radiate less efficiently. Hence, they are apt to be at a higher temperature. Conversely, surfaces with higher than average emissivities tend to be at a lower temperature. In each case the radiated signal, determined by a lower emissivity at a higher temperature or a higher emissivity at a lower temperature, has less dispersion than that of the surface temperature. The corrections which we made for the emissivities ϵ_{10} tend to increase the dispersion, but not to the extent calculated by our model.

It is also interesting to note how the reflected sky radiation and the intervening atmospheric radiation affect the radiant temperature measurements. The reflected sky radiation increases t detectable radiation, thus compensating for t nonblack surface with a larger effect for surfa with lower emissivities, and thus masking the fect of emissivity variations. The atmospheric c umn introduces an error between the surface te perature and the measured temperature th increases approximately linearly with altitu based on the experimental studies of Weiss (197

Errors associated with the corrected temperature data

The effect of increasing the mean emissivi from 0.935 to 0.965 (by 3 percent) would decrea the temperature correction terms in equation (1 by about 1.0 K. If the higher mean value for ϵ_{10} used together with an absorption coefficient A_{10} 0.293 (20 percent higher than the value used), th two effects compensate for each other, and th resulting temperature correction is within 0.1 K the values calculated in Tables 3 and 4. Erro

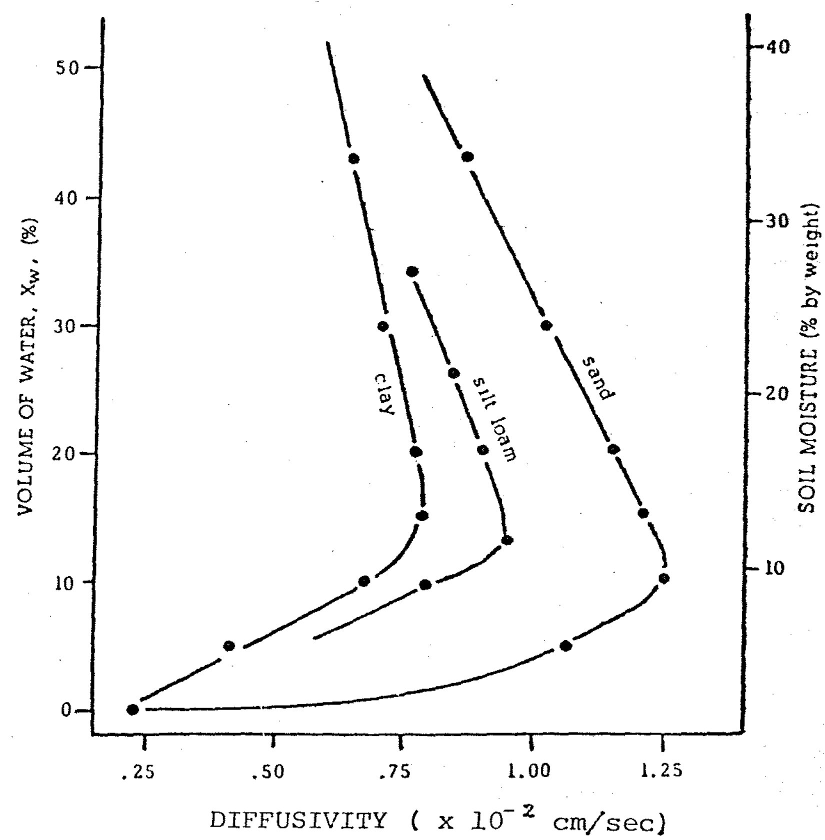

FIG. 4. Soil thermal diffusivity versus soil moisture.

…d with a ±10 K uncertainty in the aver… temperature introduce a ±0.7 K uncer… the correction for reflected sky radiation. …a ±2 K uncertainty in the temperature …by the air column introduces a ±0.7 K …ty for the associated correction term. …errors of a random nature associated with …strumentation range from 0.25 to 0.50 K. …e overall experimental uncertainties asso… with these effects, added in quadrature, …e about 1 K.

…mmarize, uncertain atmospheric condi… …uld introduce systematic errors of ±1 K. …tural temperature variations (as shown by …ndard deviations computed in Tables 3 and …e ±1 K. However, if the mean temperature were based on 100 vegetated terrain groups instead of 2 (each with about 20 temperature measurements), the mean temperature could be estimated with a precision of ±0.1 K.

This approach was used to evaluate temper-

Table 4. Input meterological modeling data to Outcalt model, October 11, 1972.*

Latitude	42.8°
Solar declination	−6.4°
Orbital radius vector	.9982
Dust	1 particle/cc
Station pressure	1018 m b
Precipitable water	9 mm
Mean diurnal temperature	9.5°C
Air humidity fraction	.48
Air wind velocity	447 cm/sec (10 mph)

* The last five values are 24-hour mean values.

Table 4. Continued.

…	Soil diffusivity (by vol) $cm^2/sec \times 10^{-2}$	Soil heat capacity cal cm^{-3} C^{-1}	Xw vol of H_2O, percent	Soil wet fraction* percent	Emissivity, ϵ'_{10}	Points	Albedo, percent	Surface roughness Z_0 cm	Exposure**	Slope, percent
…-4	.70	.66	42	33.4	.94	1-R180-4	20	2	0	0
3	.78	.53	29	23.6	.94	3	15	.9	0	0
2	.67	.68	44	34.2	.94	2	20	4	0	0
1	.63	.81	57	43.6	.94	1	15	7	0	0
…-6A	.75	.60	36	28.6	.94	2-R180-6A	15	.9	0	0
6	.69	.68	44	34.1	.94	6	18	.4	0	0
5	.77	.57	33	26.4	.94	5	22	2	0	0
4	.90	.44	20	16.4	.93	4	20	.7	0	0
3	.85	.50	26	20.9	.94	3	20	2	0	0
2	.80	.62	31	24.4	.93	2	20	2	0	0
1	.85	.50	26	20.5	.93	1	18	2	0	5
1A	.77	.57	33	26.4	.93	1A	15	12	180 (N)	6
…-11	.75	.60	36	28.0	.94	3-R180-11	22	3	135 (NW)	1.5
11A	.75	.60	36	28.0	.93	11A	18	7	180 (N)	6
10	.75	.59	35	27.5	.93	10	22	.8	135 (NW)	1.5
9	.76	.56	32	25.4	.94	9	18	12	135	1.5
8	.72	.63	39	29.2	.94	8	20	4	135	1.5
7	.75	.60	36	28.0	.93	7	18	.8	135	1.5
…de 6A	.83	.51	27	21.6	.95	in shade 6A	18	70	135	1.5
…ed >6	.68	.69	45	35.3	.92	not used >6	18	70	135	1.5
5	.70	.64	40	31.5	.94	5	12	9	135	1.5
4	.70	.64	40	31.7	.92	4	15	9	135	4
3	.65	.70	46	36.6	.92	3	18	.9	135	4
2	.70	.64	40	31.8	.93	2	12	9	135	4
1	.70	.65	41	32.8	.93	1	22	.4	135	4
…180-1A	.65	.73	49	38.0	.94	4-R180-1A	20	1.1	135	2
1A1	.75	.59	35	46.3	.92	1A1	20	7	135	2
1B	.75	.61	37	29.2	.92	1B	22	1.0	135	2
2	.75	.59	35	27.8	.94	2	18	1.1	135	2
3	.75	.60	36	28.5	.93	3	18	.9	135	5
4	.75	.60	36	28.8	.94	4	12	12	135	5
5	.85	.50	26	20.1	.93	5	12	6	135	5
6	.70	.64	40	31.8	.93	6	20	1.1	180 (N)	1
5-R180-1	.65	.73	49	38.1	.94	5-R180-1	12	7	180	1
1B	.67	.69	45	34.9	.92	1B	13	9	180	1
2	.70	.64	40	31.8	.94	2	13	9	180	1
3	.70	.64	41	32.6	.94	3	12	7	180	1

* Measured soil moisture by weight.
** Exposure 0° = south increases to 180° in both east and west directions, positive when directed west of south.

ature variations associated with changing elevations (Del Grande, 1975) as shown in Figure 3. The data analyzed were based on the Scipio Center survey discussed in this paper. Del Grande discerned the temperature rise from 292.1 $\pm$0.1 K to 292.3 $\pm$ 0.1 K at the 290 m elevation, over that at the 370 m elevation, this 0.2 $\pm$ 0.1 K mean temperature difference, found at topographic elevations differing by 80 m, resulted mainly from the expected temperature drop with increasing altitude modified by vegetation and surface moisture differences. Whereas midafternoon temperatures for localized sites smaller than 300 m^2 varied as much as 1 or 2 K from the mean temperature averaged over a larger area (for example about 100,000 m^2), the standard errors of the mean temperatures for areas of 70,000 and 160,000 m^2 were on the order of 0.1 K. A similar temperature difference of 0.2 $\pm$0.1 K would be produced by a conductive heat flow intensity of 30 $\pm$ 15 HFU. This is lower than the estimated heat flow threshold of 75 HFU believed realistic by some scientists (e.g., Watson, 1974). We believe as a result of the recent studies that it is feasible to identify conductive heat flows of 30 $\pm$ 15 HFU or lower.

COMPUTATION OF "NORMAL" TEMPERATURES

Using the surface temperature simulation model outlined above and described in detail by Outcalt (1972a), we have computed the "normal" temperatures that would be theoretically expected at each of the sample locations shown in Figure 1, providing there is no anomalous heat flow.

Estimation of surface environmental parameters

The soil thermal diffusivity was estimated from Figure 4 which was constructed from published data (Baver, 1972; Van Wijk, 1966). The soil volumetric heat capacity (C) was estimated assuming a volumetric mineral fraction (X_m) of 0.47 and a volume fraction of organic matter (X_0) of 0.04, and a variable water content (X_w), assuming a 49 percent porosity by volume. The relationship used is described in Van Wijk (1966) by De Vries and presented here as:

$$C = .46\, x_m + 0.6\, x_0 + x_w \text{ cal } cm^{-3}C^{-1}. \quad (19)$$

The volume fraction was calculated from field data assuming a bulk density of 1.3 gm/cc.

The soil wet fraction or surface relative humidity fraction was used synonymously with soil moisture percent (by weight) that was determined by laboratory analysis from samples collected i[n] the field at the time of the experiment. The ther[-] mal radiation emissivity was determined by meth[-] ods outlined above. Solar albedo was estimate[d] for the field sites from published data (Chang, 1968; Kondratyev, 1969). Aerodynamic surfac[e] roughness was estimated using an empirical rela[-] tionship developed by Kung and Lettau (se[e] Chang, 1968). Slope and exposure were collecte[d] directly from the 7½ minute U.S.G.S. quadrangl[e] of Scipio Center, N.Y. The solar declination an[d] radius vector were obtained from List (1966). A[ll] 24-hour mean meteorological data were calcu[-] lated from raw data observed at the first orde[r] NOAA/NWS station at Syracuse, N.Y.

Simulation results

The Outcalt model was evaluated using the in[-] put variables listed in Table 4. A preliminar[y] value of emissivity ϵ'_{10}, estimated from the liter[-] ature, was used in conjunction with the othe[r] listed variables to develop a raw, simulated gray[-] body surface temperature for each site locatio[n]. Since the model simulates surface temperatur[e] values on integral hours (solar time), we com[-] puted simulated temperatures for 1500 and 160[0] hours and linearly interpolated surface temper[-] ature values for 1527 hours solar time (the calcu[-] lated solar time corresponding to a flight time [of] 1519 hours local standard mean time for Scipi[o] Center on that date). As our analysis progresse[d] however, we felt that it would be valuable t[o] convert the previously simulated graybody tem[-] peratures to blackbody temperatures so that the[y] could be directly compared with the observed an[d] corrected blackbody temperatures T_b, listed i[n] Tables 2 and 3. To avoid having to recompute al[l] the simulated temperatures so derived, each gray[-] body temperature was multiplied by $(\epsilon'^{-1/4}_{10} - 1$ to obtain the surface blackbody temperatures. These simulated blackbody temperatures T_c ar[e] listed in Tables 2 and 3.

When these simulated surface temperatures T are compared with the observed and correcte[d] temperatures T_b for the two groups, we can se[e] that, given a modest number of samples, th[e] model appears to simulate very well the mea[n] observed temperatures for each group as shown i[n] Tables 3 and 4.

Errors associated with preparing a residual anomaly map

We have discussed above the errors associate[d] with the corrected surface temperature data.

... there are also errors that must be con-... that are associated with the results simu-... the Outcalt model. This is illustrated by ... that an overall one-to-one correlation ... observed and simulated temperature data ... the two terrain groups is not observed. ... of correlation may be due in part to ... data corrections discussed above, to lack ... of the model, or more probably, to ... the input variables that were used by the ... Values for many of the input variables had ... estimated from the literature, since these ... had not been measured at the time of over-... In an operational situation, however, they ... be measured without much difficulty, and, ... valid input data are available, the model ... been shown to simulate surface temperatures ... during the night by an *ir* scanner) ... 0.2K (Outcalt 1972b). Unfortunately, lack-... such input data measurements, there is no ... of estimating the spread of errors asso-... with the temperatures simulated in the ... work. We recognize that the closeness of ... mean simulated values to the mean observed ..., i.e., 0.01 and 0.15 K, may be fortuitous, ... the significant error about these values can be ... K, based on our analysis of errors. However, ... think that it is meaningful that a Student ... Test applied to data from both groups ... that the hypothesis that the observed and ... temperatures statistically come from ... same population, can be accepted at the 95 ... confidence level. This implies that, at least ... statistical basis, the "normal" temperature ... computed by the Outcalt model can be ... compared with the observed values to derive a ... residual anomaly map. It seems likely that as we ... more observed values and simulate more sur-... temperatures that match the geographic posi-... of the observed data, the significant error in ... group of values will be reduced. It also ap-... from our limited data that as the number of ... values from both the observed and simulated pop-... increases, the means of these populations ... converge. Whether this will prove to be the ... as more data are recorded and analyzed, and ... more simulations are run, has yet to be deter-... Accordingly, we think that the method-... discussed shows promise and considerably ... greater field and modeling efforts are warranted.

SUMMARY AND CONCLUSIONS

Our results suggest a way of utilizing *ir* data as a geophysical tool instead of a medium amenable only to photointerpretation, as is most commonly done. To do this, numerous complicating factors must be removed, i.e., the effects of surface emissivity, soil composition and soil moisture, topography, hydrology, and meteorological conditions, which can completely mask the temperature effects sought. The techniques developed herein appear to be useful in making the needed corrections to raw *ir* data, thus permitting the isolation of the true temperature anomalies sought. The steps required to accomplish this are as follows:

1) Reduce the effect of emissivity. If the emissivity ratio is constant, as appeared to be the case where the terrain had vegetative cover, equation (6) suggests that the signal ratio $(W_5/W_{10})^{1/5} = (\epsilon_5/\epsilon_{10})^{1/5}T_b$ can be used to determine the surface temperature.
2) Once the effects of emissivity have been removed from the signal, the corrections for meteorological, topographical, and ground surface conditions can be applied by simulating the "normal" surface temperatures that would be expected at each point on this terrain at the time of data collection. The residual between the observed surface temperatures and the temperatures simulated by the model can then be attributed to the anomalous conditions sought.

As an example of this, we observed that for the 18 points belonging to group 1, the mean of the *simulated* temperatures were essentially equal to the mean of the associated 18 *observed* temperature values, and that for the 16 group 2 values the difference was 0.1°C. Moreover, the simulated and the observed temperatures appear to come from the same population. This suggests to us that with a sufficiently large number of data samples recorded by airborne means, and taken within a nominal area of perhaps 500 m on a side, the means of the simulated temperatures can be made to converge on the means of the observed (and corrected) temperature values such that a true surface temperature contour map could be constructed. The construction of such a map implies that data values will be sufficiently far apart so that the usual photograph-like surface detail will be deliberately averaged out to produce a temperature map representing a large area. If all corrections have been made properly such that the significant error is small, and there is no abnormal heat flow in the area owing to near-surface geologic processes, then the residual between the observed and simulated data will approach zero. Where temperature residuals are not zero and meaningful geologic patterns can be interpreted from the residual anomaly maps, the results of our methodology suggest a potential new technique for geophysical exploration.

ACKNOWLEDGMENTS

We wish to thank Dr. Arthur H. Lachenbruch, U.S. Geological Survey, Menlo Park, Ca., Dr. John Lewis, McGill University, and Dr. Sam I. Outcalt of the University of Michigan for the many helpful discussions that we had with them during the course of the research. Additionally, we would like to thank Dr. Jules D. Friedman, U.S. Geological Survey, Denver, Colo., Donald R. Wiesnet of the National Oceanic and Atmospheric Administration, Suitland, Md., and Dr. Paul Ebert of the University of California Lawrence Livermore Laboratory for reviewing our manuscript. This work was supported in part by the Energy Research and Development Administration contract W-7405-Eng-48 and by the National Oceanic and Atmospheric Administration under contract 4-35308.

REFERENCES

Baver, L. D., et al., 1972, Soil physics (4th Ed.): New York, John Wiley and Sons.

Chang, U. H., 1968, Climate and agriculture: Chicago, Aldine Press.

Del Grande, N. K., 1975, An advanced airborne infrared method for evaluating geothermal resources: Proc. 2nd U.N. Symp. Develop. and Use of Geothermal Res., San Francisco, Ca. May 20–29.

Dickinson, D. J., 1973, Aerial infrared survey of Kawerau, Rotorua and Taupo Urban Areas: Geophys. Div., Dept. Scientific and Industrial Research, rept. no. 89, Wellington, New Zealand.

Gates, D. M., and Tantraporn, W., 1952, The reflectivity of deciduous trees and herbaceous plants in the infrared to 25 microns: Science, v. 115, p. 613–616.

Hodder, D. T., Martin, R. C., Calamai, A., and Cataldi, R., 1973, Remote sensing of Italian geothermal steam field by infrared scanning: Proc. 1st Pan Am. Sympos. on Remote Sensing, Panama City, R. P.

Kondratyev, K. Ya., 1969, Radiation in the atmosphere: New York, Academic Press.

LeSchack, L. A., Del Grande, N. K., Outcalt, S. I., Lewis, J., and Jenner, C., 1975, Correlation of dual-channel airborne IR data with soil moisture measurements: Proc. 1975 ASP-ACSM Fall Convention, Phoenix, Ariz., Oct. 26–31.

List, R., 1966, Smithsonian meteorological tables (6th Ed.): Washington, D.C., Smithsonian Institute Press.

Outcalt, S. I., 1972a, the development and application of a simple digital surface climate simulator: J. Appl Meteorol., v. 11, p. 629–636.

——— 1972b, A reconnaissance experiment in mapping and modeling the effect of land use on urban thermal regimes: J. Appl. Meteorol., v. 11, p. 1369–1373.

——— 1972c, The simulation of subsurface effec the diurnal surface thermal regime in cold reg Arctic v. 25, p. 306–308.

——— 1972d, The simulation and implications of mal plumes produced by arctic constructio smooth terrain: Arch. Met. Geoph. Biokl., ser. 20, p. 261–267.

Peck, E. L., Bissell, V. C., and Farnsworth, R. K., International Field Year for the Great Lakes borne snow reconnaissance: Interim rept. no. 1 drol. Res. Lab., Office of Hydrology, Nat Weather Service, National Oceanic and Atmosp Admin., Silver Spring, Md. 20910.

Pohn, H. A., Offield, T. W., and Watson, Ken 1974, Thermal inertia mapping from satellite crimination of geologic units in Oman: J. U.S.G.S., v. 2, p. 147–158.

Saunders, P. M., 1970, Corrections for airborne ation thermometry: J. Geophys. Res. v. 7 7596–7601.

Shaw, R. W., and Irbe, J. G., 1972, Environm adjustments for the airborne radiation thermo measuring water surface temperature: Water sources Res., v. 8, p. 1214–1225.

Tien, C. L., 1974, Atmospheric corrections for airt measurements of water surface temperature: Optics, v. 13, p. 1745–1746.

Van Wijk, W. R. (Ed.), 1966, The physics of environment (2nd Ed.): Amsterdam, North-Ho Publishing Co.

Watson, K., 1974, Geothermal reconnaissance quantitative analysis of thermal infrared im Proc. 9th Int'l Sympos. Remote Sens. Env 15–19 April, Env. Res. Inst. of Mich., Ann A Mich., v. 3, p. 1919–1926.

Weiss, M., 1971, Airborne measurements of earth face temperature (ocean and land) in the 10–1 and 8–14 μm regions: Appl. Optics, v. 10, p. 1287.

Wolfe, W. L., (Ed.), 1965, Handbook of militar frared technology: Contract Nonr 1224(12) ARPA Order 161, Of. Nav. Res., Dept. of N Washington, DC.

REFERENCES FOR GENERAL READIN(

Dawson, G. B., and Dickinson, D. J., 1970, Heat studies in thermal areas of the North Island of Zealand: Geothermics, spec. iss., v. 2, p. 466.

Hochstein, M. P., and Dickinson, D. J., 1970, Inf remote sensing of thermal ground in the Taup gion, New Zealand: Geothermics, spec. iss., v. 420.

Larsen, L. M., 1973, Detector utilization in line ners: Infrared and Optics Dept., Willow Run La tories Rept., NASA contract no. NAS9-9784, versity of Michigan.

LeSchack, L. A., Morse, F. H., Brinley, W. R., Jr., I N. G., and Ryan, R. B., 1973, Potential use o borne dual-channel infrared scanning to detect sive ice in permafrost: Permafrost: North Am trib. to 2nd Int'l Conf., Nat'l Acad. Sci., Washin D.C.

Palmason, G., Friedman, J. D., Williams, R. S., sson, J., and Saemundsson, K., 1970, Aerial inf survey of Reykjanes and Torfajokull thermal a Iceland: Geothermics spec. iss., v. 2, p. 399.

Vincent, R. K., 1973, A thermal infrared ratio im method for mapping compositional variations ar silicate rock types: Ph.D. thesis, University of M igan.

White, D. E., and Miller, L. D., 1969, Calibrati geothermal infrared anomalies of low intensi terms of heat flow, Yellowstone National Park stract): Trans. AGU, v. 50, p. 348.

mulation of subsurface ... thermal regime in cold ...
-308.
mulation and implications of ... iced by arctic construction ... h. Met. Geoph. Biokl., ser. B ...
C., and Farnsworth, R. K., ... Year for the Great Lakes ... issance: Interim rept. no. 1, ... Office of Hydrology, National ... tional Oceanic and Atmospheric ... g. Md. 20910.
T. W., and Watson, K., ... ia mapping from satellite ... ogic units in Oman: J. ... 7-158.
Corrections for airborne ... J. Geophys. Res., v. ...
e. J. G., 1972, Environmental ... airborne radiation thermometer ... face temperature: Water Re... 1214-1225.
spheric corrections for airborne ... er surface temperature: Appl. ... -1746.
). 1966, The physics of ...): Amsterdam, North-Holland ...
thermal reconnaissance from ... of thermal infrared imagery ... pos. Remote Sens. Environ., ... Inst. of Mich., Ann Arbor, ... 926.
e measurements of earth sur... n and land) in the 10-12 μm ... Appl. Optics, v. 10, p. 129...
5. Handbook of military ... ontract Nonr 1224(12) and ... Nav. Res., Dept. of Navy,

GENERAL READING

nson, D. J., 1970, Heat flow ... of the North Island of New ... pec. iss., v. 2, p. 466.
kinson, D. J., 1970, Infrared ... al ground in the Taupo re... othermics, spec. iss., v. 2, p. ...
ctor utilization in line scan... Dept., Willow Run Labora... tract no. NAS9-9784, Uni...
H., Brinley, W. R., Jr., Ryan, ... 1973, Potential use of air... red scanning to detect mas... ermafrost: North Am. con... at'l Acad. Sci., Washington,
D., Williams, R. S., Jon... n, K., 1970, Aerial infrared ... Torfajokull thermal areas, ... iss., v. 2, p. 399.
mal infrared ratio imaging ... ositional variations among ... hesis, University of Mich...
D., 1969, Calibration of ... alies of low intensity in ... stone National Park (ab... p. 348.

APPENDIX

... spectral radiant emittance W_λ, measured ... of (watts/m²)/unit wavelength, is what ... cted by an airborne ir scanning system. ... 's equation expresses W_λ as follows:

$$W_\lambda = \epsilon_\lambda C_1 \lambda^{-5}[\exp(C_2/\lambda T) - 1]^{-1}. \qquad \text{A-1}$$

... surface emissivity at a given wavelength λ,
... 3.7414×10^8, $W/m^2 \cdot \mu m^4$,
... $1.4388 \times 10^4\ \mu m \cdot K$,
... = wavelength in μm,
... = surface temperature in K.

... the scanner senses not the entire range of ... ted energy but only that energy contained in ... wavelength band for which the system is de... ed, equation (A-1) should be expressed as

$$W = \int_{\lambda_1}^{\lambda_2} \epsilon_\lambda C_1 \cdot [\exp(C_2/\lambda T) - 1]^{-1} \lambda^{-5}\, d\lambda. \qquad \text{(A-2)}$$

... simplify the mathematics, we will make the ... wing substitution:

$$y = C_2/\lambda T, \qquad \text{(A-3)}$$

... therefore, it follows that $\lambda = C_2/Ty$. By ... fferentiating,

$$\lambda^{-5} dy = -C_2^{-4} T^4 y^3 dy. \qquad \text{(A-4)}$$

... uation (A-2) can now be rewritten

$$W = \int_{y_1}^{y_2} \frac{\epsilon_\lambda C_1}{\exp(y) - 1} \cdot (-C_2^{-4} T^4 y^3)\ dy,^7 \qquad \text{(A-5)}$$

or

$$W = -\epsilon_\lambda C_1 C_2^{-4} T^4 \cdot \int_{y_1}^{y_2} \left(\frac{y^3}{\exp(y) - 1}\right) dy. \qquad \text{(A-6)}$$

Multiplying the numerator and denominator of the bracketed term by $(\exp -y)$, we have

$$\frac{y^3 \exp(-y)}{1 - \exp(-y)},$$

and

$$W = -\epsilon_\lambda C_1 C_2^{-4} T^4 \cdot \int_{y_1}^{y_2} \left(\frac{y^3 \exp(-y)}{1 - \exp(-y)}\right) dy. \qquad \text{(A-7)}$$

The term

$$\frac{\exp(-y)}{1 - \exp(-y)}$$

can be expanded in a binomial series, as

$$\exp^{-y} \sum_{m=0}^{\infty} \exp(-my)$$
$$= \exp(-y)[\exp(-0) + \exp(-y) + \exp(-2y) + \cdots \exp(-my)]$$

or

$$[\exp(-y) + \exp(-2y) + \exp(-3y) + \cdots \exp -(m+1)y]$$

which can be expressed as

$$\sum_{m=1}^{\infty} \exp(-my).$$

Equation (A-7) can now be rewritten using the above expansion and eliminating the negative sign by reversing the limits of integration as follows:

$$W = \epsilon_\lambda C_1 C_2^{-4} T^4 \cdot \int_{y_2}^{y_1} y^3 \left(\sum_{m=1}^{\infty} \exp(-my)\right) dy. \qquad \text{(A-8)}$$

Integrating equation (A-8) by parts, using the form

$$\int y^3 \exp(-my)\, dy = \frac{y^3 \exp(-my)}{-m} - \frac{3}{-m} \int y^2 \exp(-my)\, dy,^8$$

we obtain

$$W = \epsilon_\lambda C_1 C_2^{-4} T^4 \cdot \left[\sum_{m=1}^{\infty} \exp(-my_2)\left(\frac{y_2^3}{m} + \frac{3y_2^2}{m^2} + \frac{6y_2}{m^3} + \frac{6}{m^4}\right) - \sum_{m=1}^{\infty} \exp(-my_1) \cdot \left(\frac{y_1^3}{m} + \frac{3y_1^2}{m^2} + \frac{6y_1}{m^3} + \frac{6}{m^4}\right)\right]. \qquad \text{(A-9)}$$

[7] For integrations over small wavelength intervals, ϵ_λ is considered constant; λ applies to the mean wavelength.

[8] Standard Mathematical Tables, Chemical Rubber Company, 12th Ed., 1962, p. 309, Integral #354.

Equation (A-9) is a complete expansion of Planck's equation. However, it is unwieldy to evaluate for our emissivity ratio analysis.

Accordingly, we have derived an approximation of equation (A-9) that considerably simplifies the mathematics. Differentiating equation (A-1) with respect to T and holding λ constant, we obtain

$$dW_\lambda = \epsilon_\lambda C_1 \lambda^{-5} \cdot \frac{(C_2/\lambda T^2)\exp(C_2/\lambda T)}{(\exp(C_2/\lambda T) - 1)^2}\, dT. \quad \text{(A-10)}$$

Dividing equation (A-10) by W_λ, we obtain

$$\frac{dW_\lambda}{W_\lambda} = \frac{(C_2/\lambda T^2)\exp(C_2/\lambda T)}{[\exp(C_2/\lambda T) - 1]}\, dT, \quad \text{(A-11)}$$

or

$$\frac{dW_\lambda}{W_\lambda} = (C_2/\lambda T) \cdot \left[\frac{\exp(C_2/\lambda T)}{\exp(C_2/\lambda T) - 1}\right]\frac{dT}{T}. \quad \text{(A-12)}$$

The bracketed term, by multiplying and dividing by $\exp(-C_2/\lambda T)$, can be rewritten

$$\left[\frac{1}{1 - \exp(-C_2/\lambda T)}\right],$$

which is of the form $1/1 - x$, where $x = \exp(-C_2/\lambda T)$. It therefore can be expressed as a binomial expansion of the form

$$\frac{1}{1-x} = 1 + x + x^2 + \cdots x^m = \sum_{m=0}^{\infty} x^m,$$

as long as $\exp(-C_2/\lambda T) < 1$. This will be the case for the wavelengths of interest in this work. With the nominal temperature of 15°C or 288 K (recorded at the time of the field study) and for data recorded in wavelengths less than 15 μm, the bracketed term is approximately equal to unity; this is because the second and higher order terms of the expansion are much less than 1. Accordingly, Equation (1-12) can be expressed as

$$\frac{dW_\lambda}{W_\lambda} = \frac{C_2}{\lambda T}\frac{dT}{T}. \quad \text{(A-13)}$$

Since by definition, $dW_\lambda/W_\lambda \equiv dln\, W_\lambda$, and $dT/T \equiv dln\, T$, for small temperature excursions less than ± 5 K from T_0, where $T = T_0(1 \pm \Delta T/T_0) \cong T_0$, integrating equation (A-13) becomes:

$$\ln W_\lambda \Big|_{W_\lambda(T_0)}^{W_\lambda(T)} = -\frac{C_2}{\lambda}\cdot\frac{1}{T}\Big|_{T_0}^{T}, \quad \text{(A-14)}$$

$$\ln \frac{W_\lambda(T)}{W_\lambda(T_0)} = -\frac{C_2}{\lambda}\left(\frac{1}{T} - \frac{1}{T_0}\right) = -\frac{C_2}{\lambda T_0}\left(\frac{T_0}{T} - 1\right), \quad \text{(A-15)}$$

whence

$$W_\lambda(T) = W_\lambda(T_0)\exp\left(\frac{T_0}{T} - 1\right) \cdot \left(-\frac{C_2}{\lambda T_0}\right) \quad \text{(A-16)}$$

$$= W_\lambda(T_0)\left[\exp\left(\frac{T_0}{T} - 1\right)\right]^{-C_2/\lambda T_0} \quad \text{(A-17)}$$

Since T is near T_0, $(T_0/T - 1)$ is small, and we may expand the exponential obtaining

$$W_\lambda(T) = W_\lambda(T_0)\left[1 + \left(\frac{T_0}{T} - 1\right)\right]^{-C_2/\lambda T_0}, \quad \text{(A-1}$$

$$= W_\lambda(T_0)\left(\frac{T_0}{T}\right)^{-C_2/\lambda T_0}$$

$$= W_\lambda(T_0)\left[\frac{T}{T_0}\right]^{C_2/\lambda T_0} \quad \text{(A-1}$$

$$= \frac{W_\lambda(T_0)}{T_0^{(C_2/\lambda T_0)}} \cdot T^{(C_2/\lambda T_0)} \quad \text{(A-}$$

$$= C_\lambda(T_0)T^{(C_2/\lambda T_0)} \propto \epsilon_\lambda T^{(C_2/\lambda T_0)}. \quad \text{(A-}$$

For $C_2 = 14{,}388\ \mu\text{m} \cdot \text{K}$ and a nominal value $T_0 = 288$ K, $C_2/T = 49.96$, equation (21) can closely approximated by

$$W_\lambda \propto \epsilon_\lambda\, T^{50/\lambda}. \quad \text{(A-}$$

We have computed the difference for a change W_λ from $T = 288$ K to $T = 289$ K by evaluat equation (A-9), the complete expansion Planck's equation, and Equation (A-22). Co paring the results, we found that for the wa lengths of interest to us (i.e., between 5 μm and μm), equation (A-22) introduces an error of more than $\pm$ 0.04 percent. From the above, have derived a convenient expression relating radiant emittance sensed by a typical *ir* scanne the absolute surface temperature raised to power of $50/\lambda$. This power law thermal m becomes an extremely useful mechanism for hancing either the effects of emissivity or of face temperature.